Journal of Nanoparticle Research (2004) 6:577–588
DOI: 10.1007/s11051-004-3170-5

A new thermal conductivity model for nanofluids

Junemoo Koo and Clement Kleinstreuer*
*Department of Mechanical and Aerospace Engineering, Campus Box 7910, Broughton Hall 4160, Raleigh, NC 27695-7910, USA; *Author for correspondence (Tel.: +1 919-515-5261; Fax: +1 919-515-7968; E-mail:ck@eos.ncsu.edu)*

Received 20 May 2004; accepted in revised from 8 September 2004

Key words: nanofluids, effective thermal conductivity, apparent thermal conductivity, Brownian motion, interparticle potential, modeling and simulation

Abstract

In a quiescent suspension, nanoparticles move randomly and thereby carry relatively large volumes of surrounding liquid with them. This micro-scale interaction may occur between hot and cold regions, resulting in a lower local temperature gradient for a given heat flux compared with the pure liquid case. Thus, as a result of Brownian motion, the effective thermal conductivity, k_{eff}, which is composed of the particles' conventional static part and the Brownian motion part, increases to result in a lower temperature gradient for a given heat flux. To capture these transport phenomena, a new thermal conductivity model for nanofluids has been developed, which takes the effects of particle size, particle volume fraction and temperature dependence as well as properties of base liquid and particle phase into consideration by considering surrounding liquid traveling with randomly moving nanoparticles.

The strong dependence of the effective thermal conductivity on temperature and material properties of both particle and carrier fluid was attributed to the long impact range of the interparticle potential, which influences the particle motion. In the new model, the impact of Brownian motion is more effective at higher temperatures, as also observed experimentally. Specifically, the new model was tested with simple thermal conduction cases, and demonstrated that for a given heat flux, the temperature gradient changes significantly due to a variable thermal conductivity which mainly depends on particle volume fraction, particle size, particle material and temperature. To improve the accuracy and versatility of the k_{eff} model, more experimental data sets are needed.

Introduction

As first demonstrated by Choi (1995), highly conductive nanoparticles of very low volume fractions distributed in a quiescent liquid (called 'nanofluids'), may measurably increase the effective thermal conductivity of the suspension when compared to the pure liquid (Figure 1). Specifically, aluminum and copper-oxide spheres and carbon-nanotubes of an average diameter of 30 nm, in volume concentrations between 0.001% and 6% generated thermal conductivities $k_{\mathrm{nanofluid}} \leq 3k_{\mathrm{carrierfluid}}$ (Choi et al., 2001; Eastman et al., 2001; Patel et al., 2003). Thus, the use of nanofluids, for example in heat exchangers, may result in energy and cost savings and should facilitate the trend of device minituarization. More exotic applications of nanofluids can be envisioned in biomedical engineering and medicine in terms of optimal nano-drug targeting and implantable nano-therapeutics devices.

In any case, of major interest in this paper is to explore why the presence of low-concentration metallic nano-spheres in water increases the thermal conductivity. Traditional theories, such as Maxwell (1904) or Hamilton and Crosser (1962),

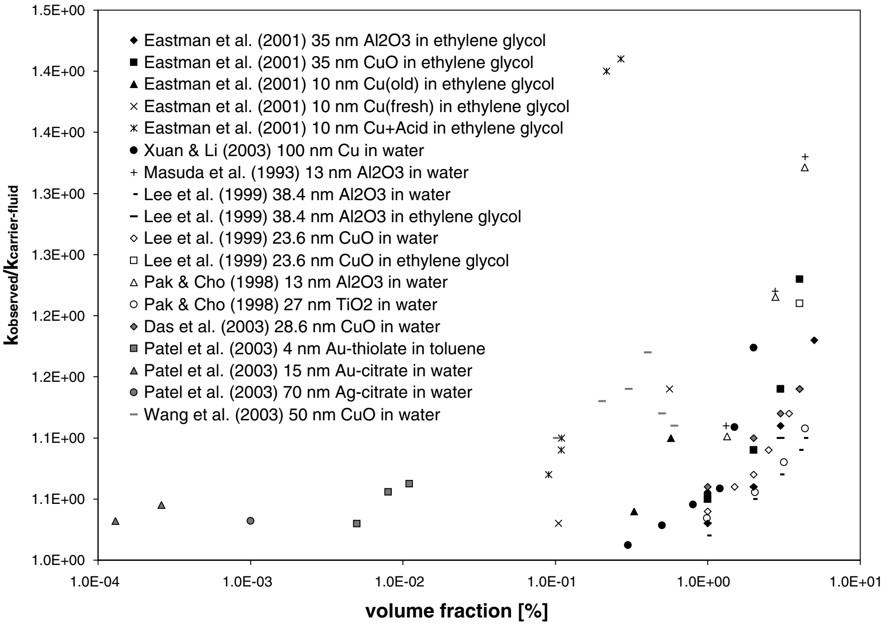

Figure 1. Experimental data sets.

cannot explain this thermal phenomenon. Thus, new assessments and mathematical models of the new apparent (or effective) thermal conductivity have been proposed. For example, Xuan and Li (2000) summarized previous experimental observations and concluded that k_{eff} was a function of both the thermal conductivities of the nano-material and carrier fluid, in terms of particle volume fraction, distribution, surface area, and shape. Keblinski et al. (2002) listed four possible explanations for the cause of an anomalous increase of thermal conductivity: Brownian motion of the nanoparticles, molecular-level layering of the liquid at the liquid/particle interface, the nature of heat transport in the nanoparticles, and the effects of nanoparticle clustering. They ruled out the possibility of the Brownian motion effect by comparing the time scales of Brownian motion and the thermal response, a point revisited in the Results section. Xue (2003) proposed a thermal conductivity model based on Maxwell's theory and average polarization theory to take care of the interface (i.e., liquid nano-layer) effect. He matched the predicted thermal conductivity values with the observed ones by changing the nano-layer thickness. Yu and Choi (2003, in press) modified the Maxwell equation and Hamilton–Crosser relation for the effective thermal conductivity of solid/liquid suspensions to include the effect of ordered nano-layers around the particles. They also matched the model with observed conductivities by adjusting the nano-layer thickness and conductivity. Bhattacharya et al. (2004) investigated the effect of particle Brownian motion by using a molecular dynamics type approach which does not consider the motion of fluid molecules and requires two experimentally determined parameters. Jang and Choi (2004) suggested an effective thermal conductivity model considering the particles' Brownian motion. They focused on the heat transfer between particles and carrier fluid, neglecting the mixing due to random particle motion. Furthermore, the validity of their thermal boundary layer thickness, which they defined as $3\delta_{\mathrm{BF}}/\mathrm{Pr}$, where $\mathrm{Pr} < O(10)$ and $\delta\mathrm{BF}$ is the diameter of the fluid molecule, is questionable when applying the continuum approach together with their Nusselt number correlation.

In this study, a new model based on kinetic theory for the effective thermal conductivity of nanofluids is proposed and compared with experimental data. The new model takes the particle dynamics into consideration and provides a means for the understanding of the more effective micro- and macroscopic energy transfer mechanisms in nanofluids. A few illustrative examples of 1-D heat conduction with nanofluids are provided.

Theory

It is postulated that the enhanced thermal conductivity of a nanofluid, when compared to conventional predictions, is mainly due to Brownian motion which produces micro-mixing. This effect is additive to the thermal conductivity of a *static* dilute suspension, i.e.,

$$k_{\mathrm{eff}} = k_{\mathrm{static}} + k_{\mathrm{Brownian}}, \tag{1}$$

where for example, according to Maxwell (1904)

$$\frac{k_{\mathrm{static}}}{k_c} = 1 + \frac{3(\frac{k_d}{k_c} - 1)\alpha_d}{(\frac{k_d}{k_c} + 2) - (\frac{k_d}{k_c} - 1)\alpha_d}, \tag{2}$$

where α_d is the particle volume fraction, k_c, the thermal conductivity of the carrier fluid and k_d is that of the particles. Since the speed of thermal wave propagation is much faster than the particle Brownian motion, the static part cannot be neglected.

Concerning temperature-dependence, Patel et al. (2003) performed experiments with suspensions of very small volume fractions, i.e., $\alpha_d < 0.001\%$, where the static part of the thermal conductivity is negligible. They observed a measurable increase of thermal conductivity even when the volume fraction was as low as 0.00013%. They also found that the thermal conductivity of the nanofluids increases with fluid temperature, which supports the importance of the Brownian motion effect (see Eq. (1)). Das et al. (2003) also observed the temperature dependence of the thermal conductivity for different type of nanofluids.

For the derivation of k_{Brownian}, we consider two nanoparticles with translational time-averaged Brownian motion, $\bar{v}$, in two different temperature fields (or cells) of extent l, where l is the average distance for a particle to travel along one direction without changing its direction due to the particle Brownian motion (see Figure 2). It should be noted that l is different from the interparticle distance due to the intervening fluid and interaction between particles and fluid molecules. For a gas, l is the same as the interparticle distance since there is no intervening medium between gas molecules. Hence, the travel time is $\Delta t = l/\bar{v}$, where (Probstein, 2003)

Table 1. Particle speed due to the Brownian effect and corresponding particle Reynolds number of Cu-nanoparticle-water suspensions

Particle size (nm)	Traveling speed (m/sec)	Re_D (–)
10	1.63	1.87×10^{-2}
100	5.15×10^{-2}	5.90×10^{-3}
1000	1.63×10^{-3}	1.87×10^{-3}

$$\bar{v} = \sqrt{\frac{18\kappa T}{\pi \rho_d D^3}}. \tag{3}$$

Here, $\bar{v}$ is the translational time-averaged speed due to the Brownian effect, κ, the Boltzmann constant, T the fluid temperature, ρ_d the particle density, and D is its diameter. Table 1 lists typical values of particle traveling speeds and corresponding Reynolds numbers.

Defining p as the probability for a particle to travel along any direction, and assuming that each of the two particle cells are in thermal equilibrium at temperatures of T_1 and T_2, respectively, these particles moving to neighboring cells will carry energy across the interface, i.e.,

$$q_{\mathrm{net}} = \frac{\Delta Q}{A\Delta t} \approx \frac{(pNm_d)c_v(T_1 - T_2)}{A\Delta t} = -\frac{pNm_d c_v \bar{v} \frac{\Delta T}{l} l}{A\bar{v}\, dt} \tag{4a}$$

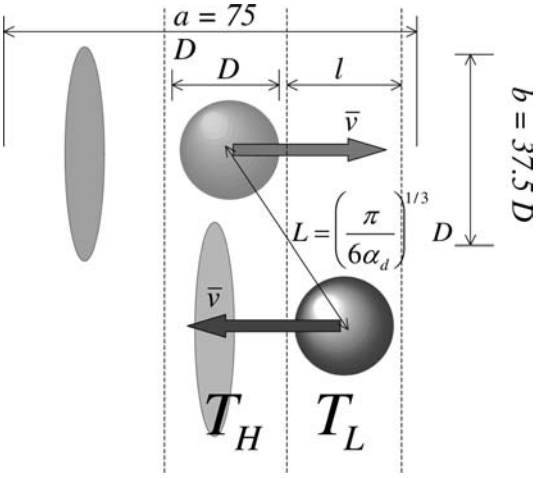

Figure 2. Schematic illustrating the particles' Brownian-motion effect on micro-mixing.

With $\frac{\Delta T}{l} \rightarrow \nabla T, N$ is the total particle number in a cell, m_d the particle mass, ρ_d is its density, and c_v is its specific heat, $m_d = \rho_d V_d, V_d$ is the particle volume, and A is the cross-sectional area of the system normal to the x-direction, $A\bar{v}\Delta t = V$, and $(NV_d)/V = \alpha_d$, we obtain

$$q_{\text{net}} \approx -p\alpha_d \rho_d c_v \bar{v} D \nabla T \tag{4b}$$

$$q_{\text{net}} = -\hat{k}_{\text{Brownian}} \nabla T. \tag{4c}$$

Here, $\hat{k}_{\text{Brownian}}$ is the added thermal conductivity due to Brownian motion of a given nano-sphere. Thus, with Eq. (3)

$$k_{\text{Brownian}} = \sqrt{\frac{18}{\pi}} p\alpha_d \rho_d c_v \sqrt{\frac{\kappa T}{\rho_d D}\frac{l}{D}}. \tag{5}$$

Clearly, as the nanoparticles *randomly* move, a portion of the surrounding fluid is affected, i.e., fluid motion and interaction occurs, leading to micro-scale mixing and heat transfer. For a quantitative assessment, we can assume steady flow in the Stokes regime (see Table 1) so that for the axial velocity field surrounding a sphere of radius R we can write (Koo, 2004).

$$\begin{aligned} \frac{v_x}{\bar{v}} &= 1 - \left[1 - \frac{3}{2}\frac{R}{r} + \frac{1}{2}\left(\frac{R}{r}\right)^3\right]\cos^2\theta \\ &\theta - \left[1 - \frac{3}{4}\frac{R}{r} - \frac{1}{4}\left(\frac{R}{r}\right)^3\right]\sin^2\theta \end{aligned} \tag{6}$$

Equation (6) can be employed to estimate the region of influence of a creeping sphere, i.e., with the 99% criterion of vanishing impact, the affected fluid volume is (Figure 2):

$$V_f = \frac{\pi}{6} a^2 b, \tag{7}$$

where $a \approx 37.5D$ is the short axes and $b \approx 75D$ is the long axes of a spheroidal body of fluid. The shape and size of affected fluid volume depends also on the particle shapes.

As a result, not just nanoparticles move around due to the Brownian effect but actually significantly larger fluid bodies, which may interact and lead to vigorous micro-mixing. Thus, Eq. (5) has to be multiplied by $(\frac{a}{D})^2 \times b/D = 105,470$ in order to encapsulate the extended Brownian motion effect. Therefore, Eq. (5) turns into

$$k_{\text{Brownian}} = 37.5^2 \times 75 \sqrt{\frac{18}{\pi}} p\beta\alpha_d \rho_d c_v \sqrt{\frac{\kappa T}{\rho_d D}\frac{l}{D}}. \tag{8}$$

Only a fraction of V_f (Eq. (7)) will travel with the particles due to the interaction among affected fluid volumes for cases, where the interparticle distance is not long enough for neighboring affected volumes to travel independently. Here, β represents the fraction of the liquid volume V_f, which travels with a particle. It will decrease with volume fraction α_d due to the viscous effect of moving particles.

Equation (8) is a result obtained from basic kinetic theory without considering the interparticle interaction, Referring to Deen (1998), it has been reported that an elementary model indicating $k_{\text{Brownian}} \sim T^{1/2}$ does remarkably well in predicting the main features of the transport properties of gases, although real gas conductivities show stronger dependences on the temperature, i.e., $k_{\text{gas}} \sim T$, instead of $\sqrt{T}$. He reported this discrepancies are largely corrected by the rigorous kinetic theory of Chapman and Enskog (Chapman & Cowling, 1951), which considers in some detail the effect of intermolecular potential energy on the interactions between colliding molecules.

For liquid–solid suspensions, the effect of interactions between solid particles are much stronger than between gas molecules, since the interparticle potential is proportional to $1/d$, where d is the interparticle distance, while it is $1/d^6$ for intermolecular potential, which decays very fast with distance. As it is observed in gases, the thermal conductivity dependence on temperature should be greater than what is predicted from elementary kinetic theory. Based on this statement, a factorial function f (T, α_d, fluid and particle properties, etc.) is added to Eq. (5) to result in

$$\begin{aligned} k_{\text{Brownian}} &= 37.5^2 \times 75 \sqrt{\frac{18}{\pi}} p\beta\alpha_d \rho_d c_v \\ &\times \sqrt{\frac{\kappa T}{\rho_d D}\frac{l}{D}} f(T, \alpha_d, \text{etc.}). \end{aligned} \tag{9}$$

The function $f(T, \alpha_d, \text{etc.})$ should depend on properties of the intervening fluid, and hence particle interactions. Traditionally, the interparticle potential can be used to take the interparticle interaction into consideration, i.e., the interparticle potential is given as

$$w(d) = -\frac{AR}{6d}, \tag{10}$$

where A is the Hamaker constant, R, the particle radius, and d is the surface distance. The Hamaker constant A for two identical phases 1 interacting across medium 3 can be described as (Israelachvili, 1992):

$$A = \frac{3}{4}\kappa T\left(\frac{\epsilon_1 - \epsilon_3}{\epsilon_1 + \epsilon_3}\right)^2 + \frac{3h\nu_e}{16\sqrt{2}}\frac{(n_1^2 - n_3^2)^2}{(n_1^2 + n_3^2)^{3/2}}, \tag{11}$$

where ϵ is the electric dipole constant, n, the refractivity, h, the Planck constant, and ν_e is the frequency where the dielectric medium has the strong absorption peak(see Table 4). For dilute cases, the thermal conductivity of the nanofluids is expected to show a relatively low dependence on particle interactions, due to the retardation effect of the interparticle potential, i.e., it is dispersion energy that suffers retardation. The complexities of the involved phenomena, make it difficult to obtain the function f theoretically if not impossible. Therefore, we decided to determine the function f from experimental data, and check whether the experimentally determined function shows the same trend with the theory, to confirm the validity of the new model. Furthermore, molecular dynamics simulations considering the particle-particle, and particle-liquid interactions should be performed to determine the average traveling distance without changing its direction l/D. Here, it is assumed that l/D=1 and the experimentally determined function f contains its effect.

Now, with the expectation value of particles to move in one direction being, 0.197 (Koo, 2004), Eq. (5) can be rewritten as

$$k_{\text{Brownian}} = 5 \times 10^4 \beta\alpha_d\rho_l c_l\sqrt{\frac{\kappa T}{\rho_d D}}f(T, \alpha_d, \text{etc.}). \tag{12}$$

Determination of the functions β *and f*

Since β is related to the particle motion, it should depend not only on volume fraction but also temperature, particle shape and material properties of particles and carrier fluid. Here we assumed that β is a function of volume fraction only, since all other dependencies can be covered with the function f. The function β can be determined with ease under the assumption that f is unity for the given conditions, i.e., temperature, material properties of particles and carrier fluid, and particle shape, because most experimental data available in the literature have been obtained at a fixed temperature. Figure 3 and Table 2 show the result obtained for water-based nanofluids. For the cases of small volume fractions, $\alpha_d < 1\%$, where the particle interaction effect is relatively less significant due to both long interparticle distance and the potential retardation effect, the function β is independent of the type of particle. In contrast, the function β depends on the type of particle in high concentration cases, $\alpha_d < 1\%$, which is found to be the result of interparticle interactions. As was expected, the function β decreased with the volume fraction α_d in most cases. It will be discussed in more detail in ‘Results and Discussion’ section.

There are not many data sets available for determining the function f. Das et al. (2003) and Patel et al. (2003) observed that their experimentally measured thermal conductivity increased with temperature. Specifically, the thermal conductivity enhancement increased by 7% for the 1% water–Al_2O_3 nanofluid, and by 15% for the 4% water–Al_2O_3 nanofluid for the temperature rise of 30 K. It increased by 20% for the 1 and 4% water–CuO nanofluid for the same temperature rise. Patel et al. (2003) did experiments with very low concentration nanofluids and they observed about 5% increase of thermal conductivity enhancement for 30 K temperature rise. Specifically, an expression *for* f (T, α_d, properties of particles and carrier fluid) in Eq. (12) was obtained from the CuO-nanofluids experimental data of Das et al. (2003). The function was assumed to vary continuously with the particle volume fraction because data for two volume concentration cases were available.

$$\begin{aligned} f(T, \alpha_d) =& (-6.04\alpha_d + 0.4705)T \\ &+ (1722.3\alpha_d - 134.63). \end{aligned} \tag{13}$$

It should be noted that the function is a linear equation because of the Taylor series truncation; but, that functional dependence can be confirmed with Eqs. (10) and (11) as well. Eq. (13) is valid for the given experimental conditions in the ranges

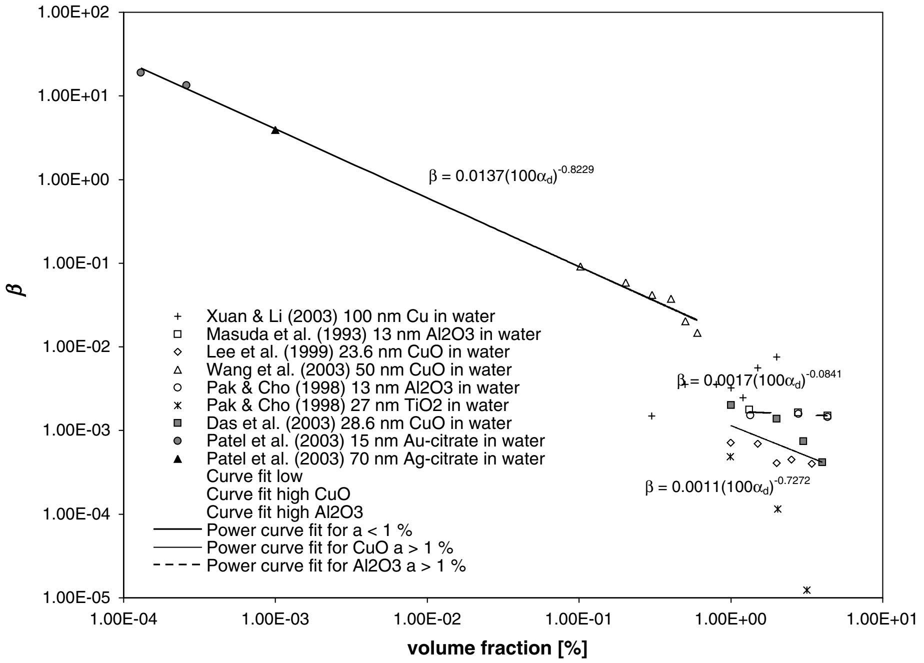

Figure 3. Comparison of β-functions obtained from experimental data.

$1\% < \alpha_d < 4\%$ and $300 < T < 325$[K]. The change of k_{Brownian} with α_d is given as

$$\begin{aligned}\frac{dk_{\text{Brownian}}}{d\alpha_d} &= 1.9318\rho_l c_l\sqrt{\frac{\kappa T}{\rho_d D}}\{0.2728\alpha_d^{-0.7272}\\ &\quad((-6.04\alpha + 0.4705)T\\ &\quad + (1722.3\alpha_d - 134.63))\\ &\quad + \alpha_d^{0.2728}(-6.04T + 1722.3)\}.\end{aligned} \tag{14}$$

The last term in the equation becomes negative and increases with temperature, which explains the thermal conductivity reduces near $x=1$ m in ‘Results and Discussion’ section.

We investigated other transport mechanisms, such as thermophoresis and fluid thermal energy, potentially contribution to enhanced thermal conductivities of nanofluids, and found that they are negligible (Koo, 2004). The results for typical nanoparticles (CuO, $D=10$ nm, $\alpha_d=1\%$) suspended in water are given in Table 3.

Table 2. Comparison of augmented thermal conductivities

Type of particles	β	Remarks
Au-citrate, Ag-citrate and CuO	$0.0137\ (100\alpha_d)^{-0.8229}$	$\alpha_d<1\%$
CuO	$0.0011\ (100\alpha_d)^{-0.7272}$	$\alpha_d>1\%$
Al_2O_3	$0.0017\ (100\alpha_d)^{-0.0841}$	$\alpha_d>1\%$

Results and discussion

Higher thermal conductivities due to Brownian motion effect

In a quiescent suspension, nanoparticles move randomly and thereby carry relatively large volumes of surrounding liquid with them. This micro-scale interaction may occur between hot and cold

Table 3. Comparison of augmented thermal conductivity parameters

Parameter type*	Increase (%)
$k_{\text{Brownian}}/k_{\text{water}}$	1950
$k_{\text{TP}}/k_{\text{water}}$	0.07
$k_{\text{PTE}}/k_{\text{water}}$	0.80

*k_{Brownian} is given with Eq. (5), k_{TP} is due to thermophoresis, and k_{PTE} is due to particle thermal energy.

regions, resulting in a lower local temperature gradient for a given heat flux compared with the pure liquid case. Thus, as a result of Brownian motion, the effective thermal conductivity, k_{eff}, increases, which results in a lower temperature gradient for a given heat flux (see Figure 4). Furthermore, at elevated suspension temperatures, the Brownian motion effect increases and higher k_{eff}-values arise (see Figures 4 and 6) as was experimentally observed by Patel et al. (2003) and Das et al. (2003). As stated in the Introduction, Keblinski et al. (2002) argued that the thermal diffusion time scale is much smaller than Brownian diffusion time scale by an order of 10^2 for 10 nm particle suspensions. However, considering the effective complex particle-plus-liquid volume to be $\beta 37.5^2 \times 75 \times V_d$ and taking a typical value of β as 0.01 (see Figure 3), the two time scales have about the same order of magnitude, and hence Brownian motion becomes a very important mechanism for augmented heat transfer.

Additional confirmation of the importance of the Brownian effect can be deduced when different carrier fluids and nano-material have been used. For example, Lee et al. (1999) found thermal conductivity improvement in ethylene glycol based nanofluids when compared to water based ones. Xie et al. (2002) observed that the thermal conductivity augmentation ratio decreases with an increase in base liquid thermal conductivity. Xie et al. (2003) compared the effective thermal conductivity of distilled-water (DW)-, ethylene-glycol(EG)-, and decene (DE)-based carbon nanotube-suspensions and observed the following result.

$$k_{\mathrm{DW}} < k_{\mathrm{EG}} < k_{\mathrm{DE}} \tag{15}$$

Lee et al. (1999) also observed that the ethylene glycol based nanofluids showed higher thermal conductivity than the water based ones.

The thermal conductivity due to Brownian motion is not explicitly related to the fluid thermal conductivity, while the static part of the effective thermal conductivity is strongly dependent on it (see Eq. (2)). The thermal conductivity of the three liquids are 0.611, 0.252, and 0.145 (W/mK), respectively. Moreover, their thermal capacities ($\rho_l c_l$), to which the thermal conductivities due to Brownian motion are proportional, are 4153, 2674, and 1700 (kJ/m^{3}K), respectively. Using the fact that

$$\frac{k_{\mathrm{Brownian}}}{k_{\mathrm{static}}} \sim \frac{\rho_l c_l}{k_c}. \tag{16}$$

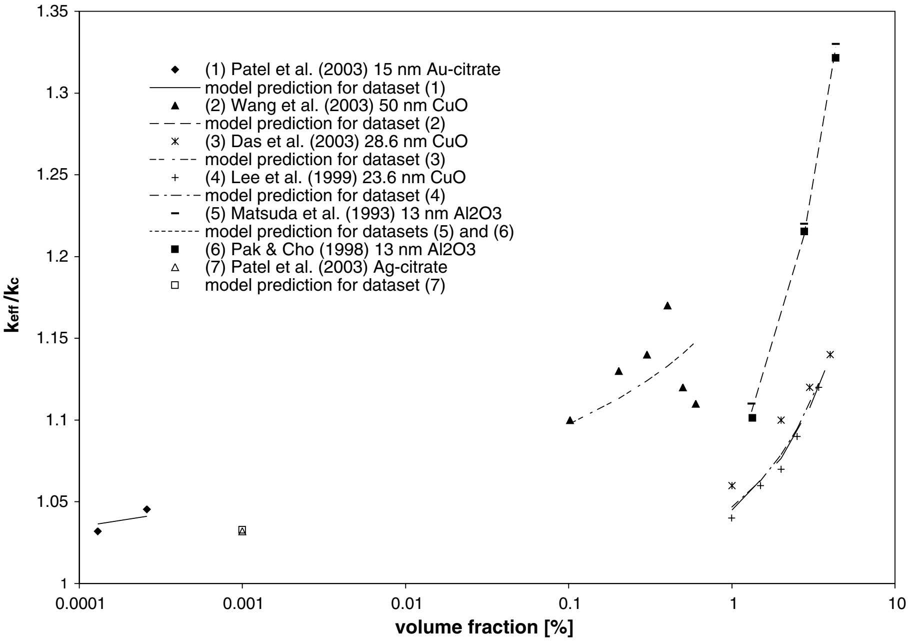

Figure 4. Comparison of model predictions with experimental data sets.

Table 4. Parameter values for different materials (see Eq. (11))

Phase material	ϵ	n	A_0^*
Cu	inf		3.11×10^{-21}
Al_2O_3	4.5	1.761	2.48×10^{-21}
CuO	18.1	2.6	1.24×10^{-21}
TiO_2	86	2.6	4.06×10^{-24}
Water	80.4	1.33	
Ethylene glycol	37.0		
Decene	2.2	2.2	

$^*A_0$ is the first term in Eq. (11).

The ratio among the three suspensions is

$$\left(\frac{k_{\text{Brownian}}}{k_{\text{static}}}\right)_{\text{DW}} : \left(\frac{k_{\text{Brownian}}}{k_{\text{static}}}\right)_{\text{EG}} : \left(\frac{k_{\text{Brownian}}}{k_{\text{static}}}\right)_{\text{DE}} = 0.58:0.91:1, \tag{17}$$

which explains their observations and merits the effect of Brownian motion.

Interparticle interactions for high concentrations, i.e., $\alpha_d > 1\%$, cases

As mentioned in Theory section, the intermolecular interaction becomes more important for suspensions with high particle concentrations. The interparticle potentials for suspensions of nanoparticles of $d > 10$ nm, the non-retarded part of the potential is most important (Israelachvili, 1992). Table 4 shows the Hamaker constants of the non-retarded term(cf. Eq. (11), where $A_0 = \frac{(3)}{(4)} kT \left(\frac{(\epsilon_1-\epsilon_3)}{(\epsilon_1+\epsilon_3)}\right)^2$). Clearly, the β-function, when $\alpha_d > 1\%$ (see Figure 3) for the four particle materials, i.e., Cu, Al_2O_3, CuO, and TiO_2, encapsulates the same relative magnitute trend as A_0 (see Table 4). This supports our explanation that the effective thermal conductivity for α_d>1% is mainly affected by interparticle interactions. As shown with Eq. (11), interparticle interaction becomes more important when the difference in electric dipole constants between particle and carrier fluid increases. It also depends on the volume fraction α_d and the particle size (cf. Eq. (10)). Compared to the potential between (gas) molecules which is inversely proportional to d^6, the cluster potential impacts long range. Figure 5 shows the effect of the exponent in the potential on the impact distance; lower exponent cases show longer impact distance. Especially, the attractive part is inversely

Figure 6. Comparisons of temperature, temperature gradient, and effective thermal conductivity profiles.

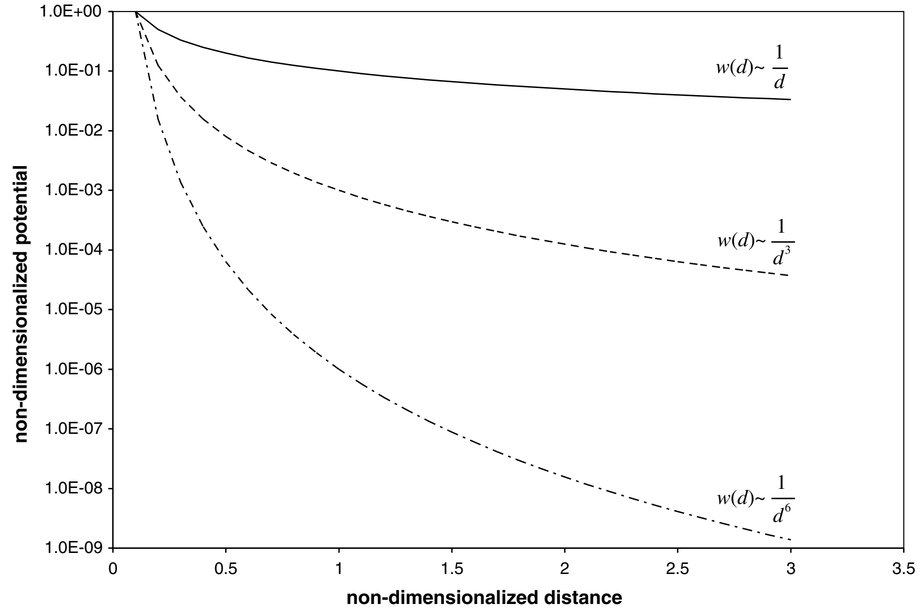

Figure 5. Comparison of effect of the exponent in the intermolecular potential on impact distance.

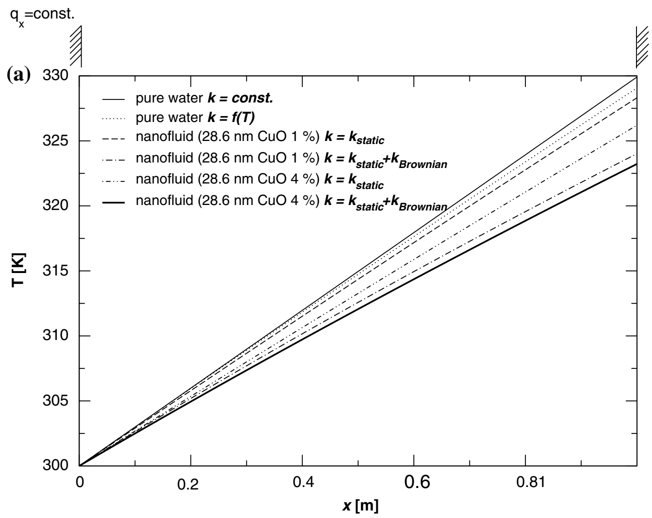
q_x=const.
(a)
pure water k = const.
pure water k = f(T)
nanofluid (28.6 nm CuO 1 %) k = k_static
nanofluid (28.6 nm CuO 1 %) k = k_static+k_Brownian
nanofluid (28.6 nm CuO 4 %) k = k_static
nanofluid (28.6 nm CuO 4 %) k = k_static+k_Brownian
T [K]
330
325
320
315
310
305
300
0
0.2
0.4
0.6
0.81
x [m]

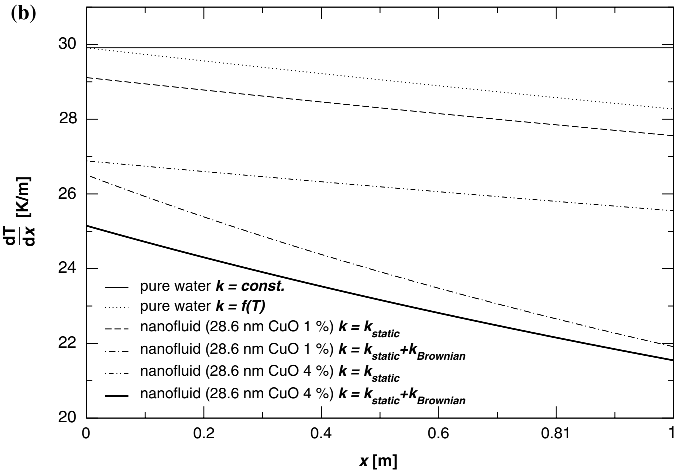
(b)
dT/dx [K/m]
30
28
26
24
22
20
pure water k = const.
pure water k = f(T)
nanofluid (28.6 nm CuO 1 %) k = k_static
nanofluid (28.6 nm CuO 1 %) k = k_static+k_Brownian
nanofluid (28.6 nm CuO 4 %) k = k_static
nanofluid (28.6 nm CuO 4 %) k = k_static+k_Brownian
0
0.2
0.4
0.6
0.81
1
x [m]

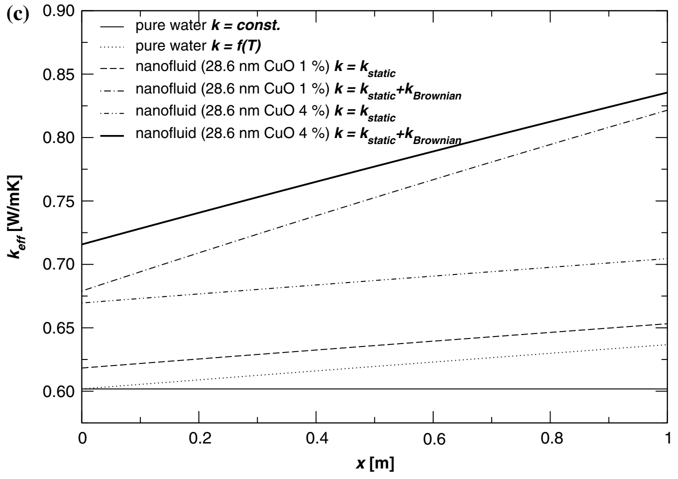
(c)
k_eff [W/mK]
0.90
0.85
0.80
0.75
0.70
0.65
0.60
pure water k = const.
pure water k = f(T)
nanofluid (28.6 nm CuO 1 %) k = k_static
nanofluid (28.6 nm CuO 1 %) k = k_static+k_Brownian
nanofluid (28.6 nm CuO 4 %) k = k_static
nanofluid (28.6 nm CuO 4 %) k = k_static+k_Brownian
0
0.2
0.4
0.6
0.8
1
x [m]

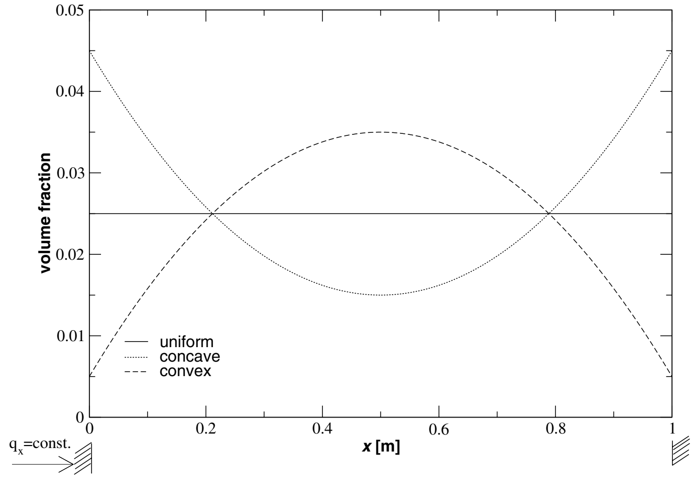

Figure 7. Volume fraction Profiles.

proportional to the surface distance itself. Israelachvili (1992) reported that large distance contributions to the interaction disappear only for values of the exponent in the potential greater than 3. But for the exponent smaller than 3, the contribution from more distant molecules will dominate over that of near by molecules. The measured gas thermal conductivities show stronger temperature dependence *(k~T)* compared to the predicted values using kinetic theory. More rigorous treatment of kinetic theory including the effect of intermolecular potential energies can correct the discrepancies for gases (Deen, 1998). Stronger temperature dependence compared to gases is expected in liquids due to long-reaching potential.

Examples of heat conduction in nanofluids

The axial conduction heat flux component can be expressed as

$$q_x = -k_{\mathrm{eff}}\frac{dT}{dx}. \tag{18}$$

A sample problem is solved considering a steady state without internal heat generation, constant heat flux case. Figure 6 shows the profiles of temperature, temperature gradient, and effective thermal conductivity in pure water and uniform nanofluids of different particle volume fractions for a heat flux of 18 (W/m^2)] in a 1-D system. The temperature at x=1 m is lower by 7 K for the 4% nanofluid case compared to the pure water of constant thermal conductiviy case. From the data in Table 2, the thermal conductivity due to Brownian effect is proportional to $\alpha_d^{0.2728}$, while the static part is proportional to α_d. The higher contribution of Brownian motion in the nanofluid of α_d=1% compared to that of the 4% case, makes the temperature difference very small. Referring to temperature gradient and thermal conductivity graphs, the difference between the two nanofluids becomes smaller at higher temperatures due to the Brownian effect. The temperature gradients, considering the temperature dependence of the thermal conductivity, show decreasing trends since the thermal conductivity increases with temperature as indicated in Eq. (12).

It is possible for particles to have nonuniform distributions due to the interaction between particles and wall. Particles could be denser either near a wall or the center of conduits. Figure 7 shows three different particle distribution profiles with an average volume fraction of 2.5%. The resulting profiles of temperature, temperature gradient, and the effective thermal conductivity are shown in Figure 8. The temperature profiles for all cases are almost the same, while $\nabla T(x)$ and $k_{\mathrm{eff}}(x)$ change and differ significantly. The thermal conductivity with a concave α_d-distribution is higher near x=0, whereas that for the uniform

Figure 8. Effect of volume fraction change on temperature-, temperature gradient-, and effective thermal conductivity-profiles.

(a)

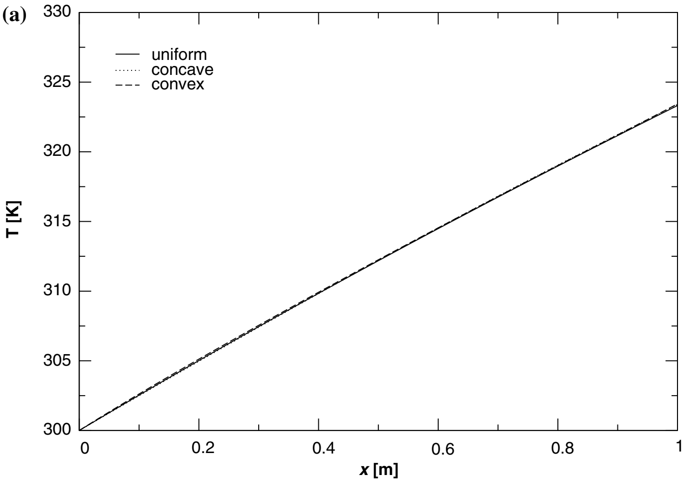
330
325
320
315
310
305
300
T [K]
0
0.2
0.4
0.6
0.8
1
x [m]
uniform
concave
convex

(b)

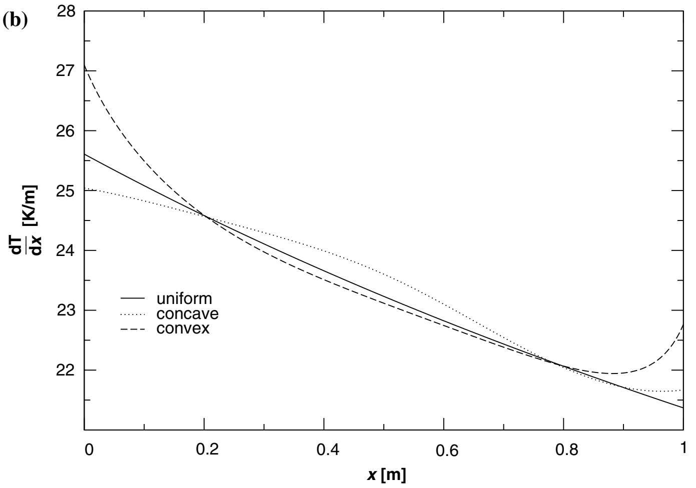
28
27
26
25
24
23
22
dT/dx [K/m]
0
0.2
0.4
0.6
0.8
1
x [m]
uniform
concave
convex

(c)

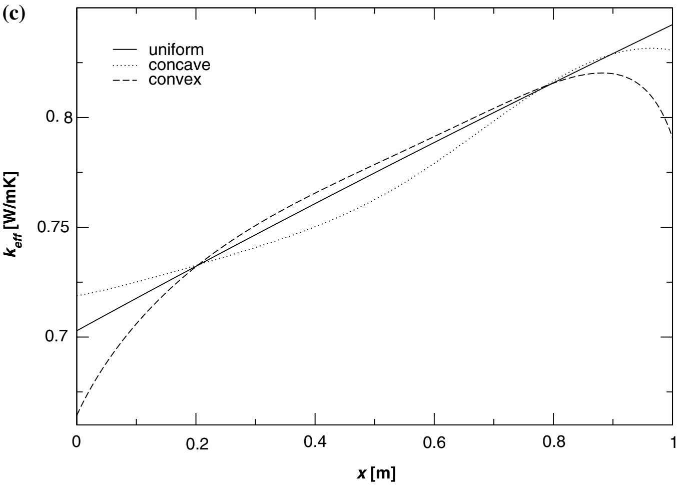
0. 8
0.75
0.7
k_{eff} [W/mK]
0
0.2
0.4
0.6
0.8
1
x [m]
uniform
concave
convex

distribution case is highest near $x=1$ m. This is the impact of the particle volume fraction on the Brownian effect part of the effective thermal conductivity.

Conclusions

A new thermal conductivity model for nanofluids has been developed, which takes the effects of particle size, particle volume fraction and temperature dependence as well as properties of base liquid and particle phase into consideration by considering surrounding liquid traveling with randomly moving nanoparticles. The time scales for such a complex particle-liquid body creating micro-mixing and local heat transfer were found to be of about the same magnitude, which manifests the efficient energy transport due to Brownian motion. The strong temperature dependence was attributed to the long impact range of interparticle potential. In the new model, the Brownian motion effect was found to become more effective at higher temperatures as observed experimentally.

The effect of interparticle potential was found to be very important for dense nanofluids, i.e., $\alpha_d > 1\%$ by comparing the experimentally obtained thermal conductivities with the calculated interparticle potentials. The electric dipole constant was observed to be a very important parameter influencing the interparticle potential and hence resulting in a particle-type dependence of the thermal conductivity.

The new model was tested with simple thermal conduction cases, and demonstrated that for a given heat flux, the temperature gradient changes significantly due to a variable thermal conductivity, which mainly depends on particle volume fraction, particle size, particle material and temperature. To improve the accuracy and versatility of the k_{eff} model, more experimental data sets are needed.

References

Bhattacharya P., S.K. Saha, A. Yadav, P.E. Phelan & R.S. Prasher, 2004. Brownian dynamics simulation to determine the effective thermal conductivity of nanofluids. J. Appl. Phys. 95(11), 6492–6494.

Chapman S. & T.G. Cowling, 1951. Mathematical Theory of Non-Uniform Gases. 2nd edn. Cambridge University Press, Cambridge, UK.

Choi, S., 1995. Enhancing thermal conductivity of fluids with nanoparticles. FED 231, 99–103.

Choi S., Z. Zhang, W. Yu, F. Lockwood & E. Grulke, 2001. Anomalously thermal conductivity enhancement in nanotube suspensions. Appl. Phys. Lett. 79(14), 2252–2254.

Das S., N. Putra, P. Thiesen & W. Roetzel, 2003. Temperature dependence of thermal conductivity enhancement for nanofluids. J. Heat Trans. 125, 567–574.

Deen W.M., 1998. Analysis of Transport Phenomena. Oxford University Press, New York, NY.

Eastman J., S. Choi, S. Li, W. Yu & L. Thompson, 2001. Anomalously increased effective thermal conductivities of ethylene glycol-based nanofluids containing copper/nanoparticles. Appl. Phys. Lett. 78, 718–720.

Hamilton R. & O. Crosser, 1962. Thermal conductivity of heterogeneous two-component systems. I & EC Fundamentals 125(3), 187–191.

Israelachvili J., 1992. Intermolecular and Surface Forces. 2nd edn. Academic press, Amsterdam.

Jang, S.P. & S.U.S. Choi, 2004. Role of Brownian motion in the enhanced thermal conductivity of nanofluids. Appl. Phys. Lett. 84(21), 4316–4318.

Keblinski P., S. Phillpot, S. Choi & J. Eastman, 2002. Mechanisms of heat flow in suspensions of nano-sized particles (nanofluids). Int. J. Heat Mass Transfer 45, 855–863.

Koo J., 2004. Computational Nanofluid Flow and Heat Transfer Analyses as Applied to Micro-syslems, PhD Thesis. North Carolina State University, Raleigh, NC.

Lee S., S. Choi, S. Li & J. Eastman, 1999. Measuring thermal conductivity of fluids containing oxide nanoparticles. J. Heat Transfer 121, 280–289.

Maxwell J., 1904. A Treatise on Electricity and Magnetism. 2nd edn. Oxford University Press, Cambridge, UK.

Patel H., S. Das, T. Sundararajan, A. Sreekumaran, B. George & T. Pradeep, 2003. Thermal conductivities of naked and monolayer protected metal nanoparticle based nanofluids: Manifestation of anomalous enhancement and chemical effects. Appl. Phys. Lett. 83(14), 2931–2933.

Probstein R., 2003. Physicochemical Hydrodynamics. 2nd edn. Wiley, Inc., Hoboken, NJ.

Xie H., H. Lee, W. Youn & M. Choi, 2003. Nanofiuids containing multiwalled carbon nanotubes and their enhanced thermal conductivities. J. Appl. Phys. 94(8), 4967–4971.

Xie H., J. Wang, T. Xi, Y. Liu, F. Ai & Q. Wu, 2002. Thermal conductivity enhancement of suspensions containing nanosized alumina particles. J. Appl. Phys. 91(7), 4568–4572.

Xuan Y. & Q. Li, 2000. Heat transfer enhancement of nanofluids. Int. J. Heat Fluid Flow 21, 58–64.

Xue Q., 2003. Model for effective thermal conductivity of nanofluids. Phys. Lett. A 307, 313–317.

Yu W. & S. Choi, 2003. The role of interfacial layers in the enhanced thermal conductivity of nanofluids: A renovated maxwell model. J. Nano. Res. 5, 167–171.